Conformation of a Polyfluorene Derivative in Solution

Libin Wu and Takahiro Sato*

Department of Macromolecular Science, Osaka University and CREST of Japan Science and Technology Corporation, 1-1 Machikaneyama-cho, Toyonaka, Osaka 560-0043, Japan

Hong-Zhi Tang†

CREST of Japan Science and Technology Corporation, 4-1-8 Hon-cho, Kawaguchi, Saitama 332-0012, Japan

Michiya Fujiki

Graduate School of Materials Science, Nara Institute of Science and Technology (NAIST) and CREST of Japan Science and Technology Corporation, 8916-5 Takayama, Ikoma, Nara 630-0101, Japan

Received March 19, 2004; Revised Manuscript Received May 28, 2004

ABSTRACT: The molecular weight and temperature dependencies of the intrinsic viscosity [η] were investigated for poly{2,7-[9,9-bis((*S*)-3,7-dimethyloctyl)]fluorene} (PDMOF) in tetrahydrofuran (THF). By analyzing the [η] data in terms of the touched-bead wormlike chain model, we estimated the persistence length q of PDMOF. It is 9.5 nm at 20 °C and slightly increases with decreasing temperature. The results of q were compared with the theoretical ones calculated on the basis of the broken wormlike chain (BWC), rotational isomeric state (RIS), and freely rotating chain (FRC) models. The BWC model for helical polymer chains gave q much larger than the experimental values, when the excess free energy ΔG_r of the helix reversal for PDMOF was assumed to be comparable to those for typical synthetic helical polymers reported so far. On the other hand, the FRC model slightly underestimated the experimental q. A good fit to the experimental q was obtained for a simple RIS model where each monomer unit takes independently four rotational states, right- and left-handed 5/2 and 5/1 helical states, and its bond angle fluctuates slightly.

Introduction

π-Conjugated polymers have interesting electrical and optical properties, which make them very attractive as potential replacements for conventional inorganic semiconductors.[1−9] Polyacetylene and its derivatives are typical examples, and polyfluorene derivatives have recently attracted increasing interests as candidates for organic light-emitting diode with high quantum yield, high hole mobility, and excellent thermal, chemical, and photochemical stabilities.[10,11]

Because the conjugation restricts the internal rotation about their main-chain bonds, those polymers are also expected to possess nonflexible chain nature or sometimes helical nature in their global conformation, which provide us additional interesting properties, e.g., liquid crystallinity and chiroptical properties. For example, polyacetylene derivatives bearing chiral side chains were demonstrated to have strong helical nature leading to very unique chiroptical properties.

More recently, some interesting circular dichroism (CD) and circularly polarized electroluminescence (CPEL) behavior were reported for optically active polyfluorene derivatives. Oda et al.[12,13] observed strong CD and CPEL for spin-coated films of some polyfluorenes bearing chiral alkyl side chains after annealing. Tang et al.[14,15] reported temperature-dependent CD of a polyfluorene derivative with the stereocenter at the β-position in the alkyl side chains in solution. Those reports imply helical nature in the polyfluorene chain.

The CD of optically active polyfluorenes is not usually strong enough to study their helical conformation in solution.[15] In the present study, we have investigated the helicity of the polyfluorene chain by viscometry. The helical nature of the polymer chain is reflected on the global conformation, and the intrinsic viscosity [η] of the polymer chain in solution is a useful quantity to characterize the chain global conformation. Comparing molecular weight and temperature dependencies of [η] with some relevant polymer chain models, we have discussed the local helical conformation of the polymer chain in solution.

In this study, we chose poly{2,7-[9,9-bis((*S*)-3,7-dimethyloctyl)]fluorene} (PDMOF, Scheme 1). This is one of the optically active polyfluorenes which Oda et al.[12,13] studied in the spin-coated film, and its CD in solution is much weaker than that of poly{2,7-[9,9-bis((*S*)-2-methyloctyl)]fluorene} previously studied by Tang et al.[15]

Experimental Section

Polymer Fractions and Solvent. Dibromofluorene monomer bearing two (*S*)-3,7-dimethyloctyl substitutes was polymerized in hot mixture of toluene and *N*,*N*-dimethylformamide (DMF) using a zerovalent nickel reagent by the Yamamoto coupling reaction, and the end-termination was accomplished using 2-bromofluorene.[15] The polymer was divided into nine fractions (S2-0−S2-8) by size-exclusion chromatography (SEC) with two columns of Shodex KF2006M and using 40 °C toluene as the eluent. Five fractions were chosen for the following sedimentation equilibrium and viscosity experiments. The solvent THF was distilled under calcium hydrate as a desiccant.

Sedimentation Equilibrium. THF solutions of five PDMOF fractions were studied by sedimentation equilibrium, using a Beckman-Coulter Optima XL-I ultracentrifuge, equipped with a Rayleigh interferometer with 675 nm light emitted from a diode laser. The temperature was chosen to be 20 °C, and

† Present address: Department of Chemistry, North Carolina State University, Raleigh, NC 27695-8204.

10.1021/ma0494535 CCC: $27.50
Published on Web 07/10/2004

Scheme 1

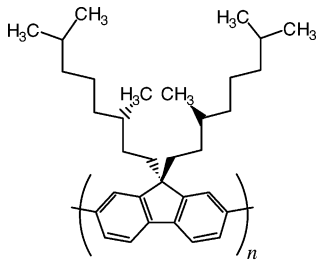

PDMOF

aluminum 12 mm double-sector cells were used. The height of the solution column was adjusted to ca. 1.5 mm, and the rotor speed was chosen in the range from 11 000 to 39 000 rpm depending on the molecular weight.

The apparent molecular weight M_{app} and the Q value were calculated from the equations[16,17]

$$M_{app} = \frac{2RT(c_b - c_a)}{\omega^2(r_b^2 - r_a^2)c_0(1 - \bar{v}\rho_0)}$$

$$Q = \frac{(c_b - c_a)^2}{(r_b^2 - r_a^2)c_0[(\partial c/\partial r^2)_{r=r_b} - (\partial c/\partial r^2)_{r=r_a}]} \qquad (1)$$

where r_b and r_a are the distance from the center of revolution to the cell bottom and meniscus, respectively, c_b and c_a are polymer mass concentrations at r_b and r_a, respectively, under the centrifugal field, which are estimated by interferometry with the specific refractive index increment $\partial n/\partial c$; ω is the angular velocity, $\bar{v}$ is the partial specific volume of the polymer, ρ_0 is the solvent density, c_0 is the polymer concentration of the solution at $\omega = 0$, and RT is the gas constant multiplied by the absolute temperature. The concentration gradients $\partial c/\partial r^2$ at r_a and r_b in eq 2 were estimated graphically. The weight-average and z-average molecular weights M_w and M_z and the second virial coefficient A_2 were determined from M_{app} and Q using the equations

$$\frac{1}{M_{app}} = \frac{1}{M_w} + 2A_2\bar{c} + O(\bar{c}^2)$$

$$Q = \frac{M_w}{M_z}[1 + 2A_2M_w\bar{c} + O(\bar{c}^2)] \qquad (2)$$

where $\bar{c}$ is the average concentration given by $(c_a + c_b)/2$.

Densitometry and Refractometry. Densities ρ and excess refractive indices Δn of THF solutions of PDMOF were measured at 20 °C as a function of the polymer concentration c to obtain the partial specific volume $\bar{v}$ and the specific refractive index increment $\partial n/\partial c$ necessary to analyze sedimentation equilibrium data. While the former measurement was made with an oscillation U-tube densitometer (Anton-Paar, DMA5000), the latter measurement was performed with a differential refractometer (Ohtsuka Electronics, DRM-1020) at 675 nm. The results of $\bar{v}$ and $\partial n/\partial c$ were 1.032 cm^3/g and 0.169 cm^3/g, respectively.

Viscometry. Viscosities of THF solutions of five PDMOF fractions were measured by using conventional Ubbelohde-type capillary viscometers at 20 °C. The Huggins and Mead−Fuoss plots were used to determine the intrinsic viscosity $[\eta]$ and the Huggins coefficient k'. For fraction S2-2, viscosities of its THF solution were also measured from −20 to 20 °C by the same way to determine $[\eta]$ and k' as functions of the temperature.

Other Measurements. Circular dichroism (CD) and UV−vis absorption spectra for dilute THF solutions of PDMOF fractions were recorded simultaneously on a JASCO J-725 spectropolarimeter equipped with a liquid nitrogen-controlled quartz cell with a path length of 0.5 cm in a cryostat at

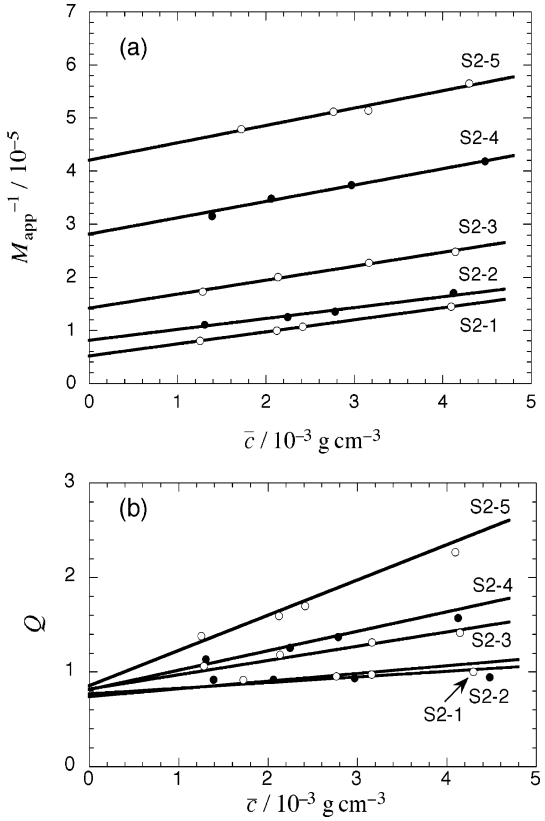

Figure 1. Plots of (a) M_{app}^{-1} vs $\bar{c}$ and of (b) Q vs $\bar{c}$ for five PDMOF fractions in THF at 20 °C.

Table 1. Molecular Characteristics of PDMOF Fractions Used

fraction	$M_w/10^4$	A_2[a]	M_z/M_w	M_w/M_n[b]	M_z/M_w[b]	$[\eta]$[c]	k'
S2-1	19.3	1.13	1.2			3.25	0.46
S2-2	12.3	1.03	1.2	1.15	1.12	2.32	0.42
S2-3	7.05	1.31	1.2	1.17	1.12	1.43	0.48
S2-4	3.56	1.50	1.3	1.19	1.15	0.65	0.49
S2-5	2.38	1.55	1.25			0.51	

[a] In units of 10^{-3} cm^3 mol/g^2. [b] Estimated by SEC. [c] In units of 10^2 cm^3/g.

wavelength of the incident light between 300 and 600 nm, ranging from 20 to −80 °C. The polymer concentration was chosen to be ca. 1×10^{-5} g/cm^3. While a strong UV absorption was observed in a range of 350−420 nm, no appreciable CD was detected for all five fractions of PDMOF in the same wavelength range.[12,15] SEC measurements were made for all the PDMOF fractions by use of the same equipment as used for the fractionation mentioned above.

Results and Discussion

Molecular Weights and Second Virial Coefficients. Figure 1 illustrates plots of M_{app}^{-1} vs $\bar{c}$ (a) and Q vs $\bar{c}$ (b) constructed from sedimentation equilibrium data. From the straight lines in Figure 1, we have determined M_w, A_2, and M_z/M_w for each fraction using eq 2. (The straight lines in panel b have been drawn with aid of A_2M_w evaluated from the plots in panel a.) Those results are listed in Table 1. The second virial coefficients A_2 estimated were 1.03×10^{-3}−1.64×10^{-3} mol g^{-2} cm^3, which indicates that THF is good solvent for PDMOF at 20 °C. Table 1 also contains SEC results of three middle fractions, where M_w/M_n and M_z/M_w were calculated with the calibration curve constructed by use of our five PDMOF fractions whose M_w were determined by sedimentation equilibrium. The values of M_z/M_w

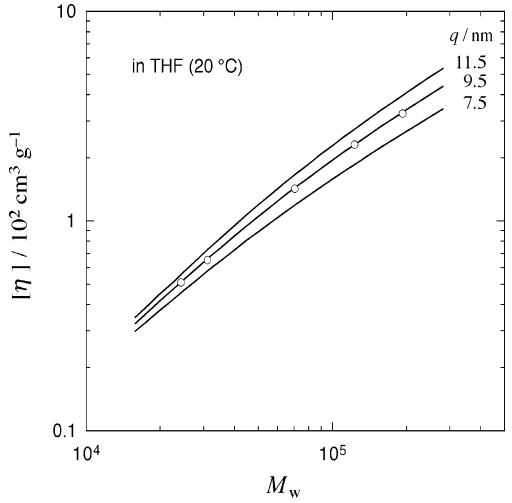

Figure 2. Molecular weight dependence of $[\eta]$ for PDMOF in 20 °C THF: circles, experimental data points; solid curve, theoretical values calculated by the theory of Yoshizaki, Nitta, and Yamakawa for the unperturbed touched-bead wormlike chain model,[18,19] with $M_L = 530$ nm^{-1}, $d_B = 1.45$ nm, $\Phi_\infty = 2.3 \times 10^{23}$ mol^{-1}, and q indicated in the figure.

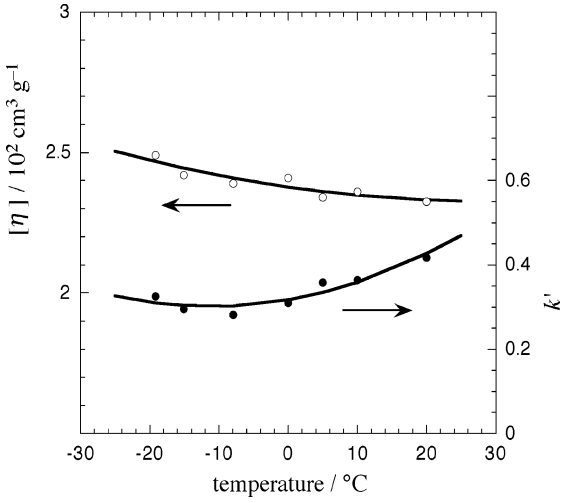

Figure 3. Temperature dependencies of $[\eta]$ and k' for fraction S2-2 ($N = 12.2$) in THF.

estimated by sedimentation equilibrium and SEC closely agree and indicate that our fractions are moderately narrow in a molecular weight distribution.

Intrinsic Viscosities. Values of the intrinsic viscosity $[\eta]$ and Huggins coefficient k' obtained for PDMOF fractions in THF at 20 °C are also summarized in Table 1. Figure 2 shows by circles the molecular weight dependence of $[\eta]$ of PDMOF in THF at 20 °C. In the double-logarithmic plot, the data points obey a curve convex downward, whose slopes are 0.97 and 0.82 below and above $M_w = 7.0 \times 10^4$, respectively. The former slope agrees with the previous result of Tang et al.,[15] and the latter slope indicates that the chain of PDMOF is not so stiff in THF.

According to the theory of Yoshizaki, Nitta, and Yamakawa for the touched-bead wormlike chain model,[18,19] $[\eta]$ can be expressed by

$$[\eta] = 6^{3/2}\Phi_\infty \frac{\langle S^2\rangle}{M}\Gamma(N;d_b) + \frac{5\pi N_A d_b^{\,2}}{12M_L} \qquad (3)$$

where Φ_∞ is the Flory−Fox constant in the coil limit, $\langle S^2\rangle$ is the mean-square radius of gyration, M is the molecular weight, N is the number of Kuhn's segments, d_b is the bead diameter, M_L is the molar mass per unit contour length, and N_A is the Avogadro constant. While $\langle S^2\rangle$ is calculated by the Benoit−Doty equation[19] for the wormlike-chain model, the explicit functional form of $\Gamma(N;d_b)$ is given by refs 18 and 19. If the persistence length q is known, N can be calculated from $N = M/2qM_L$. Thus, q, M_L, and d_b are the adjustable parameters to calculate $[\eta]$ as a function of M. Although the theoretical Φ_∞ is 2.87×10^{23} mol^{-1},[19] experimentally estimated value of Φ_∞ for flexible polymers is slightly less than this value (ca. 2.3×10^{23} mol^{-1}).[21,22] In what follows, we use a value of 2.3×10^{23} mol^{-1} for Φ_∞.

Viewing the polymer chain as a cylinder with a diameter d and the solvent as a continuous medium, we may write the partial specific volume $\bar{v}$ as

$$\bar{v} = \frac{\pi N_A d^2}{4M_L} \qquad (4)$$

Furthermore, according to Yoshizaki et al.,[18,19] the diameter d_b of the touched-bead model may be related to the cylinder diameter d by $d_b = d/0.74$. Using this relation and eq 4 as well as the experimental $\bar{v}$ (= 1.032 cm^3/g for PDMOF), we can calculate d_b from a given value of M_L.

We searched for the two adjustable parameters q and M_L leading to the best fit of eq 3 to the experimental results shown in Figure 2. The solid curves in Figure 2 indicate theoretical values of $[\eta]$ calculated by eq 3 using $q = 11.5$, 9.5, and 7.5 nm and $M_L = 530$ nm^{-1}. The middle curve perfectly fits to the experimental data points.[20] The value of d_b calculated by the above method is 1.45 nm. The Kuhn segment number N of the highest molecular weight fraction is about 20. It is known that the intramolecular excluded-volume effect is not appreciable at $N \lesssim 50$ for stiff and semiflexible polymers.[23,24] Therefore, this effect may not affect the above determinations of q, M_L, and d_b.

The q value obtained for PDMOF is close to those for other polyfluorenes bearing alkyl side chains: $q = 8.5$ nm for poly[2,7-(9,9-di-*n*-octylfluorene)] in THF (40 °C)[25] and $q = 7$ nm for poly{2,7-[9,9-bis(2-ethylhexyl)fluorene]} in toluene (20 °C).[26] These polyfluorenes are as stiff as some aromatic polyamides[27,28] and cellulose derivatives,[24,29] considerably stiffer than typical flexible polymers ($q \sim 1$ nm) but more flexible than typical rigid polymers ($q \sim 40$).[29] The result of M_L gives us the projection length h of the monomer unit along the chain contour to be 0.84 nm for the PDMOF chain with the monomer-unit molecular weight = 444. This h is close to the pitch per the monomer unit for the energetically most stable 5/2 helix (= 0.838 nm) of polyfluorene estimated by the MO calculation and molecular modeling.[30] This indicates that the local conformation of the PDMOF main chain in THF resembles this helix.

Figure 3 shows the temperature dependence of $[\eta]$ and the Huggins coefficient k' for fraction S2-2 ($N = 12.2$) in THF. The value of $[\eta]$ slightly increases with lowering temperature. On the other hand, k' tends to slightly decrease by cooling from 20 to −20 °C, and there is no indication that PDMOF forms aggregates in dilute THF solution upon cooling. Thus, the increase of $[\eta]$ may arise from the chain stiffening.

As mentioned above, the M_L value in THF is close to that for the energetically most stable 5/2 helix.[30,31] Thus, we can expect that M_L does not change upon

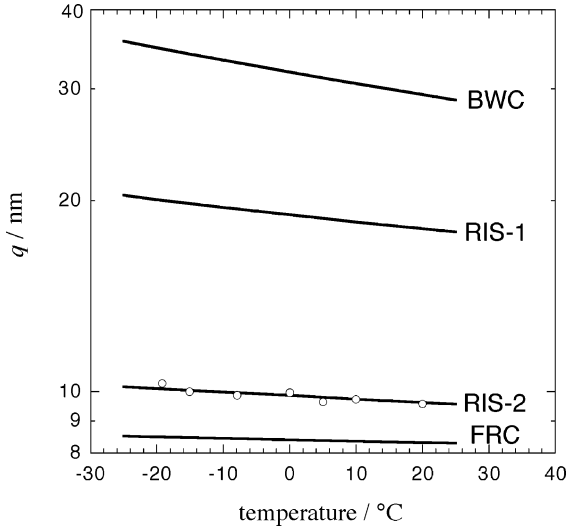

Figure 4. Temperature dependence of q for PDMOF in THF: circles, experimental data points; solid curves, theoretical values calculated by using the broken wormlike chain (BWC), rotational isomeric state (RIS), and freely rotating chain (FRC) models (see the text for detailed calculation procedures).

cooling. Furthermore, $[\eta]$ is insensitive to the value of d_b unless the axial ratio L/d_b of the chain is considerably small. Since L/d_b is 160 for fraction S2-2, we may neglect the temperature variation of d_b. Therefore, we have ascribed the temperature dependence of $[\eta]$ to the variation of q. Figure 4 presents by circles the q values estimated from $[\eta]$ of fraction S2-2 with M_L and d_b determined at 20 °C. The increase of q upon cooling is not so remarkable.

Conformation of the PDMOF Chain. Theoretically, the temperature variation of q for helical polymer chains can be estimated as follows.[32,33] On the basis of the broken wormlike-chain (BWC) model,[34] q consists of two terms of the torsional fluctuation (q_0) and of the kink due to the helix reversal. When the helical polymer chain consists of two kinds of main-chain bonds, the former is written as[35]

$$q_0 = \frac{1}{h}\left\{{b_1}^2\left(\frac{1}{2} + \left[\frac{\mathbf{T}_1\mathbf{T}_2}{\mathbf{E} - \mathbf{T}_1\mathbf{T}_2}\right]_{33}\right) + {b_2}^2\left(\frac{1}{2} + \left[\frac{\mathbf{T}_2\mathbf{T}_1}{\mathbf{E} - \mathbf{T}_2\mathbf{T}_1}\right]_{33}\right) + 2b_1b_2\left[\frac{\mathbf{T}_1}{\mathbf{E} - \mathbf{T}_1\mathbf{T}_2}\right]_{33}\right\} \quad (5)$$

where h is the pitch per the repeating unit, b_1 and b_2 are the bond lengths of the two kinds, $\mathbf{E}$ is the unit matrix, and $\mathbf{T}_i$ ($i = 1$ and 2) are the transformation matrices defined by

$$\mathbf{T}_i = \begin{pmatrix} \langle\cos\tilde{\phi}_i\rangle\langle\cos\theta_i\rangle & \langle\sin\tilde{\phi}_i\rangle & \langle\cos\tilde{\phi}_i\rangle\langle\sin\theta_i\rangle \\ \langle\sin\tilde{\phi}_i\rangle\langle\cos\theta_i\rangle & -\langle\cos\tilde{\phi}_i\rangle & \langle\sin\tilde{\phi}_i\rangle\langle\sin\theta_i\rangle \\ \langle\sin\theta_i\rangle & 0 & -\langle\cos\theta_i\rangle \end{pmatrix} \quad (i = 1, 2) \quad (6)$$

with the bond angle θ_i and internal rotation angle $\tilde{\phi}_i$, which is defined as zero at the trans state. In eq 6, $\langle\cdots\rangle$ means the thermal average with respect to $\tilde{\phi}_i$ or θ_i of the right- or left-handed helix. Incorporating the contribution of the helix reversal, we write q in the form[32,33]

$$\frac{1}{q} = \frac{1}{q_0} + \frac{1 - \cos\tilde{\theta}_V}{h\exp(\Delta G_r/RT)} \quad (7)$$

where $\tilde{\theta}_V$ is the kink angle at the helix reversal and ΔG_r is the excess free energy (per mole of the repeating unit) of the helix reversal.

Figure 5 depicts the molecular structure of a polyfluorene derivative. The structure can be specified by the bond lengths (b_1 and b_2), the bond angles (θ_1 and θ_2), and the torsional angles ($\tilde{\phi}_1$ and $\tilde{\phi}_2$). Optimum values of these parameters were estimated from crystallographic data or quantum mechanical calculations. Furthermore, fluctuations in the bond and torsional angles were estimated from the persistence length of poly(*p*-phenylene) and the internal rotation potential calculated by quantum mechanics, respectively. A detailed procedure of these estimations are explained in the Appendix.

Thus, only the unknown parameter in eqs 5−7 is ΔG_r. The circular dichroism of PDMOF is so weak that ΔG_r cannot be determined by the usual method for helical polymers.[36] Typical synthetic helical polymers (e.g., polyisocyanates, polyacetylenes, and polysilylenes) take large ΔG_r ranging from 5 to 20 kJ/mol.[33,36−38] If we choose ΔG_r to be the lower bounds 5 kJ/mol, we obtain the theoretical curve for q labeled as BWC in Figure 4, which largely overestimates the experimental results. This result indicates that the helix reversal does not cost the PDMOF chain a large excess free energy, and the chain frequently changes the sign of the rotational angle $\tilde{\phi}_2$ along the chain. That is, PDMOF should not be regarded as a regular helical polymer, being consistent with no observation of strong circular dichroism of PDMOF in THF (cf. Experimental Section).

If each bond in the polymer main chain takes independently its rotational state, we can calculate q, using the simple rotational isomeric state (RIS) model. Assuming that the monomer unit of PDMOF takes four RIS, right- and left-handed 5/2 and 5/1 helical states, where the 5/1 helical states possess a higher energy of $\Delta E_{5/1}$ than the 5/2 ones, we calculate $\langle\cos\tilde{\phi}_2\rangle$ ($\langle\sin\tilde{\phi}_2\rangle = 0$ from symmetry) and then $q = q_0$ using eqs 5 and 6. When using the theoretical value of Hong et al. for $\Delta E_{5/1}$ (= 2.26 kJ/mol), the theory gives the curve labeled as RIS-1 in Figure 4, which still overestimates the experimental data. On the other hand, the freely rotating chain (FRC) model with $\langle\cos\tilde{\phi}_2\rangle = \langle\sin\tilde{\phi}_2\rangle = 0$ provides the curve labeled as FRC in Figure 4. It slightly underestimates the experimental q.

The curve labeled as RIS-2 in Figure 4 was obtained by choosing $\Delta E_{5/1} = 0$ and β (the bond angle bending force constant; cf. eq A1) = 23.5 J/(deg^2 mol) instead of β = 49.5 J/(deg^2 mol) for the curve RIS-1. The revised value of β increases the standard deviation of the bond angles θ_1 and θ_2 from 7.0° to 10.2° at 20 °C. The choice of $\Delta E_{5/1}$ and β is however not unique, and other parameter sets equally fit to the experimental data.

In summary, we conclude from viscometry that the helical nature of PDMOF is very weak in THF. Each repeating unit in the PDMOF chain takes randomly its internal rotational state without correlation to neighboring units. As a result, PDMOF does not exhibit CD in solution. Very recently, we have observed a gradually increasing CD in THF solutions of PDMOF with slightly high concentrations upon cooling to a very low temperature (−80 °C), which indicates the formation of some chiral aggregates of PDMOF. The strong CD and CPEL

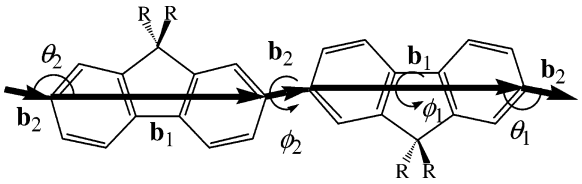

Figure 5. Geometry of a polyfluorene derivative chain.

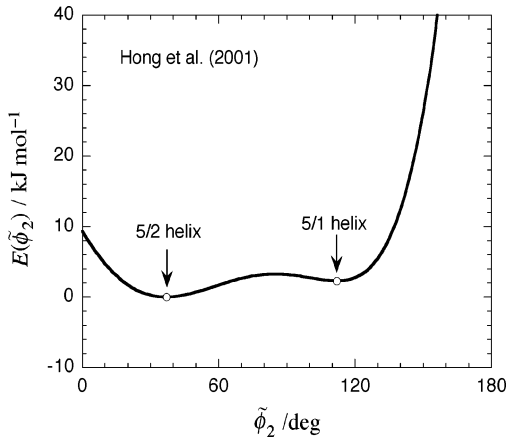

Figure 6. Internal rotation potential of polyfluorene reported by Hong et al.[31]

observed by Oda et al.[12,13] in the spin-coated film may come from such aggregates.

Acknowledgment. We are grateful to Prof. Akio Teramoto and Dr. Kazuto Yoshiba at Ritsumeikan University, who helped us with the fractionation of the PDMOF sample by SEC.

Appendix. Parameters of the Polyfluorene Chain

We can regard that the polyfluorene chain consists of two kinds of main-chain bonds $\mathbf{b}_1$ and $\mathbf{b}_2$, as shown in Figure 5. From crystallographic date,[39,40] the bond lengths are given by $b_1 = 0.69$ nm and $b_2 = 0.15$ nm and the optimum bond angles by $\theta_{1,0} = \theta_{2,0} = 168°$. The torsional angle $\tilde{\phi}_1$ is fixed at 180° due to the rigidity of the fluorene ring. On the other hand, Hong et al.[31] made a quantum mechanical calculation of the rotation energy $E(\tilde{\phi}_2)$ about $\mathbf{b}_2$ for polyfluorene. Their result is depicted in Figure 6. There are two energy minima at $\tilde{\phi}_2 = 37°$ and 112°, which correspond to (left-handed) 5/2 and 5/1 helices, respectively. The 5/1 helix is less stable by $\Delta E_{5/1} = 2.26$ kJ/mol per mole of the monomer unit than the $^5/_2$ helix. Although not shown in Figure 6, there are another minima at $\tilde{\phi}_2 = -37°$ and $-112°$ (the right-handed helices).

The averages $\langle \cos \tilde{\phi}_2 \rangle$ and $\langle \sin \tilde{\phi}_2 \rangle$ in $\mathbf{T}_2$ given by eq 6 can be calculated by the potential $E(\tilde{\phi}_2)$ given in Figure 6. On the other hand, the fluctuation of the bond angle may be described by the potential (per mole of the bond) given by

$$E_b(\theta) = \frac{1}{2}\beta(\theta - \theta_0)^2 \qquad \text{(A1)}$$

where θ_0 is the optimum bond angle and β is a bending force constant. Using this potential, we can calculate the averages $\cos \theta_2$ and $\sin \theta_2$ in $\mathbf{T}_2$ by

$$\langle \cos \theta \rangle = \cos \theta_0 \exp(-RT/2\beta),$$
$$\langle \sin \theta \rangle = \sin \theta_0 \exp(-RT/2\beta) \qquad \text{(A2)}$$

Although we have no information about β for the polyfluorene chain, we may identify it with that for poly(*p*-phenylene). The poly(*p*-phenylene) backbone is linear, and the chain flexibility only comes from the fluctuation of the bond angle. Therefore, we can estimate β for poly(*p*-phenylene) from the persistence length q of the poly(*p*-phenylene) chain in solution. Petekidis et al.[41] reported q of a poly(*p*-phenylene) derivative in chloroform to be 28 nm at 25 °C, and this value gives us $\beta = 49.5$ J/(deg^2 mol). We have used the following geometrical parameters of the poly(*p*-phenylene) chain: $b_1 = 0.285$ nm, $b_2 = 0.149$ nm, $\theta_{1,0} = \theta_{2,0} = 180°$, and $\tilde{\theta}_V = 0$.[42] This force constant β yields a value of 7.0° for the standard deviation of the bond angle between $\mathbf{b}_1$ and $\mathbf{b}_2$ at 25 °C.

To calculate q from eq 7, we need the kink angle $\tilde{\theta}_V$ at the helix reversal. There are two stable helical states (5/2 and 5/1 helical states) for the polyfluorene chain, so that we have four different types of helix reversals. Table 2 summarizes the results of $\tilde{\theta}_V$ for all the types calculated from the geometry of the polyfluorene chain on the basis of the two-state approximation.[32] The thermal average of $\tilde{\theta}_V$ may be made by use of $\Delta E_{5/1} = 2.26$ kJ/mol.

Table 2. Kink Angles at the Helix Reversal of the Polyfluorene Chain Taking the 5/2 and/or 5/1 Helical States

type of the helix reversal	$\tilde{\theta}_V$/deg[a]
5/2 (right-handed) ↔ 5/2 (left-handed)	8.0
5/1 (right-handed) ↔ 5/1 (left-handed)	34.3
5/2 (right-handed) ↔ 5/1 (left-handed)	21.1
5/1 (right-handed) ↔ 5/2 (left-handed)	21.1

[a] Calculated on the basis of the two-state approximation using geometrical parameters of the polyfluorene chain mentioned in the Appendix.

References and Notes

(1) Burroughes, J. H.; Bradley, D. D. C.; Brown, A. R.; Marks, R. N.; Mackay, K.; Friend, R. H.; Burns, P. L.; Holmes, A. B. *Nature (London)* **1990**, *347*, 539.
(2) Pei, Q.; Yang, Y.; Yu, G.; Zhang, C.; Heeger, A. J. *J. Am. Chem. Soc.* **1996**, *118*, 3922.
(3) Hide, F.; Schwartz, B. J.; Diaz-Garcia, M. A.; Heeger, A. J. *Synth. Met.* **1997**, *91*, 35.
(4) Kraft, A.; Grimsdale, A. C.; Holmes, A. B. *Angew. Chem., Int. Ed.* **1998**, *37*, 402.
(5) Yang, J.-S.; Swager, T. M. *J. Am. Chem. Soc.* **1998**, *120*, 11864.
(6) Friend, R. H.; Gymer, R. W.; Holmes, A. B.; Burroughes, J. H.; Marks, R. N.; Taliani, C.; Bradley, D. D. C.; Dos Santos, D. A.; Bredas, J. L.; Logdlund, M.; Salaneck, W. R. *Nature (London)* **1999**, *397*, 121.
(7) Gonzalez-Ronda, L.; Martin, D. C.; Nanos, J. I.; Politis, J. K.; Curtis, M. D. *Macromolecules* **1999**, *32*, 4558.
(8) McQuade, D. T.; Pullen, A. E.; Swager, T. M. *Chem. Rev.* **2000**, *100*, 2537.
(9) Arias, A. C.; MacKenzie, J. D.; Stevenson, R.; M. Halls, J. J.; Inbasekaran, M.; Woo, E. P.; Richards, D.; Friend, R. H. *Macromolecules* **2001**, *34*, 6005.
(10) Neher, D. *Macromol. Rapid Commun.* **2001**, *22*, 1365.
(11) Tang, H.-Z.; Fujiki, M.; Zhang, Z.-B.; Torimitsu, K.; Motonaga, M. *Chem. Commun.* **2001**, 2426.
(12) Oda, M.; Nothofer, H.-G.; Lieser, G.; Scherf, U.; Meskers, S. C. J.; Neher, D. *Adv. Mater.* **2000**, *12*, 362.
(13) Oda, M.; Meskers, S. C. J.; Nothofer, H.-G.; Scherf, U.; Neher, D. *Synth. Met.* **2000**, *111−112*, 575.
(14) Tang, H.-Z.; Fujiki, M.; Sato, T. *Macromolecules* **2002**, *35*, 6439.
(15) Tang, H.-Z.; Fujiki, M.; Motonaga, M. *Polymer* **2002**, *43*, 6213.

(16) Fujita, H. *Foundation of Ultracentrifugal Analysis*; Wiley-Interscience: New York, 1975.
(17) Terao, K.; Terao, Y.; Teramoto, A.; Nakamura, N.; Fujiki, M.; Sato, T. *Macromolecules* **2001**, *34*, 4519.
(18) Yoshizaki, T.; Nitta, I.; Yamakawa, H. *Macromolecules* **1988**, *21*, 165.
(19) Yamakawa, H. *Helical Wormlike Chains in Polymer Solutions*; Springer-Verlag: Berlin, 1997.
(20) The uniqueness of the wormlike-chain parameters determined was checked by the procedure of Bushin et al.[43] and Bohdanecky,[44] although not shown here.
(21) Fujita, H. *Polymer Solutions*; Elsevier: Amsterdam, 1990.
(22) Hirao, T.; Sato, T.; Norisuye, T.; Teramoto, A.; Masuda, T.; Higashimura, T. *Polym. J.* **1991**, *23*, 925.
(23) Norisuye, T.; Fujita, H. *Polym. J.* **1982**, *14*, 143.
(24) Kasabo, F.; Kanematsu, T.; Nakagawa, T.; Sato, T.; Teramoto, A. *Macromolecules* **2000**, *33*, 2748.
(25) Grell, M.; Bradley, D. D. C.; Long, X.; Chamberlain, T.; Inbasekaran, M.; Woo, E. P.; Soliman, M. *Acta Polym.* **1998**, *49*, 439.
(26) Fytas, G.; Nothofer, H. G.; Scherf, U.; Vlassopoulos, D.; Meier, G. *Macromolecules* **2002**, *35*, 481.
(27) Motowoka, M.; Fujita, H.; Norisuye, T. *Polym. J.* **1978**, *10*, 331.
(28) Sakurai, K.; Ochi, K.; Norisuye, T.; Fujita, H. *Polym. J.* **1984**, *16*, 559.
(29) Sato, T.; Teramoto, A. *Adv. Polym. Sci.* **1996**, *126*, 85.
(30) Lieser, G.; Oda, M.; Miteva, T.; Meisel, A.; Nothofer, H.-G.; Scherf, U.; Neher, D. *Macromolecules* **2000**, *33*, 4490.
(31) Hong, S. Y.; Kim, D. Y.; Kim, C. Y.; Hoffmann, R. *Macromolecules* **2001**, *34*, 6474.
(32) Sato, T.; Terao, K.; Teramoto, A.; Fujiki, M. *Macromolecules* **2002**, *35*, 2141.
(33) Sato, T.; Terao, K.; Teramoto, A.; Fujiki, M. *Polymer* **2003**, *44*, 5477.
(34) Mansfield, M. L. *Macromolecules* **1986**, *19*, 854.
(35) Ashida, Y.; Sato, T.; Morino, K.; Maeda, K.; Okamoto, Y.; Yashima, E. *Macromolecules* **2003**, *36*, 3345.
(36) Lifson, S.; Andreola, C.; Peterson, N. C.; Green, M. M. *J. Am. Chem. Soc.* **1989**, *111*, 8850.
(37) Okamoto, N.; Gu, H.; Nakamura, Y.; Sato, T.; Teramoto, A. *Macromolecules* **1996**, *29*, 2878.
(38) Morino, K.; Maeda, K.; Okamoto, Y.; Yashima, E.; Sato, T. *Chem.—Eur. J.* **2002**, *8*, 5112.
(39) Destri, S.; Pasini, M.; Botta, C.; Porzio, W.; Bertini, F.; Marchio, L. *J. Mater. Sci.* **2002**, *12*, 924.
(40) Leclerc, M.; Ranger, M.; Belanger-Gariepy, F. *Acta Crystallogr.* **1998**, *C54*, 799.
(41) Petekidis, G.; Vlassopoulos, D.; Galda, P.; Rehahn, M.; Ballauff, M. *Macromolecules* **1996**, *29*, 8948.
(42) Delugeard, Y.; Desuche, J.; Baudour, J. L. *Acta Crystallogr.* **1976**, *B32*, 702.
(43) Bushin, S. V.; Tsvetkov, V. N.; Lysenko, E. B.; Emel'yanov, V. N. *Vysokomol. Soedin.* **1981**, *A23*, 2494.
(44) Bohdanecky, B. *Macromolecules* **1983**, *16*, 1483.

MA0494535